

Application of the Monte Carlo Method for Radiation Exchange in Spacecraft

JOCHEN DOENECKE*

Delft University of Technology, Delft, The Netherlands

The calculation of radiative interchange factors using the Monte Carlo Method is treated for a general enclosure in which blockage of direct radiation can occur. Techniques for reducing computer time are described. Foremost of these techniques is that whereby, prior to the statistical process, the facing of one surface to another is calculated and stored in six matrices. Diffuse emission and mixed diffuse-specular reflectivity of five types of surfaces are programmed. Illustrative examples confirm that the error caused by the finite size of the surfaces does not occur, whereas this error has to be taken into account in other methods. Calculations, including a rough error analysis, on a 20-node model show that even when the number of trials is reduced from 400 to 100, the equilibrium temperatures are still more precise than those obtained when radiative exchange is determined in another manner. The computer runs took, at most, twenty minutes. An approximate method of subdividing very complex enclosures is presented in order to further reduce computer time.

Nomenclature

A	= area
B	= absorption factor, fraction of radiation leaving one surface and being absorbed by another surface
\mathbf{B}	= vector representing a ray
N	= number of trials or rays per area
n	= number of surfaces in enclosure
P	= point on emitting surface
$R1 \dots R7$	= random numbers
S	= point on receiving surface
T	= temperature, °K
\mathbf{V}	= vector from surface i to surface j
xyz	= fixed coordinate system
$x'y'z'$	= local coordinate system
α	= absorptivity for solar radiation
ϵ	= emissivity or absorptivity for infrared radiation
ρ	= reflectivity
σ	= Stefan-Boltzmann constant

Subscripts

d	= diffuse component
i	= of surface i
j	= of surface j
ij	= from surface i to surface j
is	= from surface i to space
s	= specular component
w	= of imaginary wall

Superscripts

'	= with respect to $x'y'z'$ system; of side of imaginary wall facing subenclosure I
"	= of side of imaginary wall facing subenclosure II

Introduction

THE calculation of radiative heat transfer in vacuum is one of the basic problems for the design and development of spacecraft. Howell and Siegel have dealt with this problem thoroughly.^{1,2} Various methods have been proposed for the diffuse case, for specularly reflecting surfaces,³ for mixed diffuse-specular reflectivities,⁴ and for the dependence on direction.⁵ All these methods are difficult to apply, however, in the general case of a complex enclosure. Generally, radiation from one surface is not received uniformly by another

surface, necessitating either a very fine subdivision of the enclosure whereby we have to deal with large matrices, or the solution of integral equations, usually by numerical methods, also requiring a fine subdivision of each surface into increments. Blockage of direct radiation between two surfaces by one or several other surfaces also presents a difficulty.

The Monte Carlo method might seem to be the most attractive for the general case. The basic applicability of this method was confirmed in Refs. 6-9. All these examples, however, are relatively simple, and the problem still exists as to whether the method can also be applied for complex enclosures without the computer program becoming very complicated and/or the running time becoming excessive. This paper presents a general program and techniques which reduce computer time.

Examples show that even for complex geometries the computer time can be kept reasonable.

Problem Statement and Solution by Monte Carlo

The net radiative energy E_i at a surface i of a general open enclosure of n surfaces can be written in the form (see Nomenclature and Ref. 10):

$$E_i = \sigma A_i \epsilon_i B_{is} T_i^4 - \sigma \sum_{j=1}^n A_j \epsilon_j B_{ji} (T_j^4 - T_i^4) \quad (1)$$

where B_{is} is the fraction of radiation leaving i and escaping into space and B_{ji} is the absorption factor between any other surface j and surface i . The problem consists of determining the $n \times (n+1)$ matrix of absorption factors, where the surface $(n+1)$ represents the black space, so that the net heat fluxes can be calculated by Eq. (1). This matrix can be calculated directly by the Monte Carlo method, providing the following advantages as compared with other methods: 1) It obviates the need to calculate the geometrical view factors. 2) It eliminates the error normally caused by the finite size of the surfaces: a finer subdivision of the enclosure as prescribed by the nodes of the thermal mathematical model is not necessary (see examples below). 3) It makes for uncomplicated inclusion of blockage (see Table 1). 4) It requires little additional effort for treating dependence of radiation on direction and wavelength.

A B_{ij} factor is determined as follows by Monte Carlo. N random points are chosen on each surface. A ray of arbitrary direction is traced from each point. The path of each ray, that represents an 'energy bundle' or 'photon' (see, for instance, Refs. 7 and 8), is followed until the ray is absorbed

Received December 14, 1972; revision received April 2, 1973.

Index categories: Radiation and Radiative Heat Transfer; Thermal Modeling and Experimental Thermal Simulation.

* Senior Research Scientist, Department of Aerospace Engineering.

by another surface or escapes from the system into space. The absorption factor is then $B_{ij} = L_j/N$, where L_j is the number of rays absorbed by j .

Seven random numbers, all distributed uniformly between 0 and 1 are used to simulate the path of a ray until the first reflection. Two random numbers, $R1$ and $R2$, determine a random point on an emitting surface i by expressing mathematically that each random number R divides the emitting surface by a line into two parts, the ratio of which is $R/(1-R)$. The intersection of two lines defines the random point. Random numbers, $R3$ and $R4$, determine the direction of the ray. A fifth random number, $R5$, can be used to determine the fate of the ray when it strikes surface j . The reflectivity ρ is composed of a diffuse part ρ_d and a specular part ρ_s , so that $\alpha + \rho_d + \rho_s = 1$, where α = absorptivity (= emissivity if only gray radiation is considered). The decision regarding the fate of the ray can be made as follows: 1) $0 < R5 < \alpha$: the ray is absorbed. 2) $\alpha < R5 < \alpha + \rho_d$: the ray is reflected diffusely. 3) $\alpha + \rho_d < R5 < 1$: the ray is reflected specularly.

In case 1 the two surfaces i and j , between which the ray travelled, are recorded in order to determine L_j . In cases 2 and 3 the point of impingement is determined and the path of the ray is followed further. In case 2 random numbers, $R6$ and $R7$, are therefore required. In case 3 the direction of the reflected ray is calculated directly. The ray is followed until case 1 occurs or until it leaves the enclosure.

It is in fact advantageous to produce random numbers at seven locations in a general computer program (see below). We verified by means of chi-square tests¹¹ that the distribution and sequence of these numbers were sufficiently random.

Techniques for Improving the Method

Prior to the statistical process the facing of one surface to another was calculated. Points P on an 'emitting' surface i and points S on a 'receiving' surface j were selected (Fig. 1) and vectors from all points P to all points S were calculated and normalized to unity. The components of the normalized vectors V were expressed with respect to a fixed coordinate system xyz in which all surfaces were either defined or found after coordinate transformations. The largest and smallest components of V were selected and stored in six matrices, $V_{x,\max}$, $V_{y,\max}$, $V_{z,\max}$, $V_{x,\min}$, $V_{y,\min}$, $V_{z,\min}$, the row and column of which characterize surfaces i and j , respectively. In order to be certain of obtaining the largest and smallest components of the unit vectors V describing all possible interconnections of i and j , the points P and S only need to be chosen in the case of flat surfaces on the contours of i and j , but in the case of curved surfaces they must also be chosen within the surfaces and have sufficient density. The surfaces i and j were therefore scanned in four loops. Two integers, K and L , define P , and two integers, M and N , define S (Fig. 1).

During the statistical process each ray leaving i is represented by a vector B , which is also normalized. An impingement on j is possible only when the components of B , B_x , B_y ,

and B_z , are such that all the following three inequalities are fulfilled:

$$\begin{aligned} V_{x,\min}(i,j) &\leq B_x \leq V_{x,\max}(i,j) \\ V_{y,\min}(i,j) &\leq B_y \leq V_{y,\max}(i,j) \\ V_{z,\min}(i,j) &\leq B_z \leq V_{z,\max}(i,j) \end{aligned} \quad (2)$$

By means of inequalities (2), one can ascertain whether or not a point of impingement S on j will be obtained after a parallel shift of B over the whole surface i . The six matrices are calculated only once and stored in the computer; the time required for this plus the time for applying Eqs. (2) is negligible compared with the time for the calculation of points of impingement. If Eqs. (2) are not fulfilled for a particular vector B , one can immediately check to see if an impingement is possible on the next surface j , thereby saving time usually spent on the ray-tracing subroutine. The probability that Eqs. (2) will be fulfilled is inversely proportional to the average number of surfaces seen (fully or partially) by i . Eqs. (2) represent a generalization of the method given in Ref. 12, which is applicable only for plane surfaces, whereas Eqs. (2) can also be used for curved surfaces.

Even when Eqs. (2) are fulfilled, S can lie outside j : vectors B_1 and B_2 (Fig. 1), when shifted parallel to B_1^* and B_2^* , respectively, give an impingement point inside j , and thus fulfill Eqs. (2). However, only the point of impingement of B_1 itself lies inside j , whereas that of B_2 lies outside. It is sometimes necessary to test for certainty in regard to the position of the point of impingement. Five types of surfaces are treated: trapeziums, annular- or ring-surfaces, cylindrical-, conical-, and spherical-surfaces or segments of the latter four.

If j is a trapezium, another inequality can be used before the certainty test is made. The vectors from S to the points 1 to 4 are calculated (Fig. 2). The scalar products between these vectors give the cosines of the four angles λ_1 , λ_2 , λ_3 and λ_4 . In order to check if the sum of these angles is 360° , in which case S certainly lies inside j , the angles have to be calculated from their cosines. Since this requires relatively much computer time, one first tests if

$$\sum_{k=1}^4 \cos \lambda_k > 0.5 \quad (3)$$

If this equation is fulfilled, S will lie outside j and one can go on to the next surface to look for a point of impingement. Thus Eq. (3) eliminates further surfaces of trapezoidal form, for which the four angles would otherwise have to be calculated. Equation (3) can be derived by calculating the maximum of the sum of the cosines for S inside j .

In the case where the emitting surface i is flat, the time required for the calculation of the direction of an emitted ray can be reduced by storing a 3×3 transformation matrix $[T]$ in the computer. The values of $R3$ and $R4$, together with the equations of spherical coordinates, give the vector B' , which represents the emitted ray with respect to a local coordinate system $x'y'z'$. The x' and y' axes are chosen in the plane of surface i , and z' is chosen normal to i (Fig. 1). The unit vectors i' , j' , k' along the $x'y'z'$ axes, respectively, are calculated. The components of i' , j' and k' give the elements of $[T]$, and B' can be transformed into the xyz system by

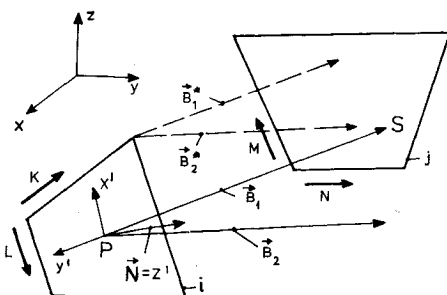


Fig. 1 Calculation of matrices that define how surfaces face each other.

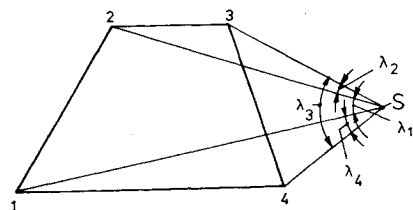


Fig. 2 Test for impingement on a trapezium.

$\mathbf{B} = [T]\mathbf{B}'$. $[T]$ is stored as long as random points are produced on a particular surface i . $[T]$ has to be calculated again for each point P in the case where i is curved; \mathbf{k}' is then taken normal to an element dA_i of i . \mathbf{B} and the normal to the surface at the point of impingement S are used to calculate a new coordinate system at S . This system is then used to calculate the direction of the reflected ray for diffuse as well as for specular reflection.

The number of trials, N , needed to obtain a result with a certain precision is (see, for instance, Ref. 7 or 8):

$$N = 2\eta(1 - p)/(pd^2) \quad (4)$$

where p = exact result (for $N \rightarrow \infty$), d = relative error = δ/p , δ = absolute error, η = probability factor: $P = \text{erf}(\eta)$ (for instance, for $\eta = 2.178$ there is a probability of 99.7% that the relative error will not be greater than d). Equation (4) means that N is independent of the dimension of the problem. Disregarding multireflections in our case gives a 4-dimensional problem ($R1$ to $R4$ are used). One can calculate that when determining a volume in a 4-dimensional space by testing if N uniformly distributed points are inside or outside this volume, the required number N can indeed be larger than that which would be obtained by Eq. (4) (for the same η , p and d). When distributing the points uniformly, however, one can be more sure than with Monte Carlo that the result is never very wrong even when N is low. We have therefore also programmed a method in which the points P on i are chosen at centers of a uniform grid and in which a uniform bundle of rays is sent from each point P .

Unit hemispheres are constructed over P . On each hemisphere points are chosen as uniformly distributed as possible and the rays pass from P through these points. We have found that this way of choosing a uniform bundle gives more precise results than choosing the rays such that they all represent the same fraction of energy. When a ray is diffusely reflected, Monte Carlo is always used to find the new direction. The examples confirmed that the method of uniform rays is useful in the case of nearly black surfaces when multiple reflections are insignificant.

The 'stratified sampling' technique,¹³ was also tried in an effort to improve the program. The emitting surfaces were subdivided and the absorption factors from each area section to a receiving surface j were calculated and averaged. A clear improvement could not be observed (see below). The considerable additional programming effort does not seem to be worthwhile. It is always possible to subdivide a critical surface finer, and calculate for each section the absorption factors, although only their averages are later used in a thermal analyzer program.

The technique of 'antithetic variates'¹³ was also tried. This technique implies that a negative correlation is created between two statistical results, so that their average is closer to the exact result. N random numbers give a first result. Each number R is then replaced by $1-R$, giving a second result. If the first result lies above the exact value, the second one will lie below it and vice versa. When considering, for instance, parallel sunlight which falls on a unit square and which is simulated by random rays one can demonstrate that this technique can, depending on the position of j , either give an improvement or a detriment. We applied this technique to a few examples, but do not particularly recommend it.

Computer Program

Table 1 gives a rough outline of our program, which considers blockage. By 'codes' in item 1 we mean certain input such as integers that define the number of passages in the different loops, an array which specifies if the active area of a curved surface is inside (concave) or outside (convex) and a matrix $MT(i, j)$ that specifies whether or not direct radiation is possible between i and j . If an element of $MT(i, j) = -1$,

there is no direct exchange between i and j , if $MT(i, j) = 0$, there is partial blockage; if $MT(i, j) = 1$, there is no blockage. In case of doubt regarding the possibility of blockage, one has to put $MT(i, j) = 0$. In the case where $MT(i, j) = -1$ the calculation process skips from item 7 to 14 and for $MT(i, j) = 1$, the process skips over item 11, providing a reduction in the running time.

Loop 3 is programmed since it might be desirable to do several runs for one geometry. For instance, one might wish to calculate the absorption of parallel sunlight into a cavity, as well as the interchange of infrared radiation. Both cases can be calculated successively by using different surface properties. The solar radiation is simulated by parallel rays of random origin from a trapezoidal surface, which has to be chosen so large that the entire opening of the cavity can receive rays. The fraction of rays that in some cases may fall outside the cavity can easily be determined. Between loops 5 and 6, two further loops can define the point P on i if i is subdivided by a uniform grid. Under item 9 several sub-routines are used in order to find the point of impingement. For spherical surfaces a numerical solution is programmed in order to calculate two unknowns from two trigonometric equations. The use of the seven random numbers $R1$ to $R7$ is also indicated in Table 1.

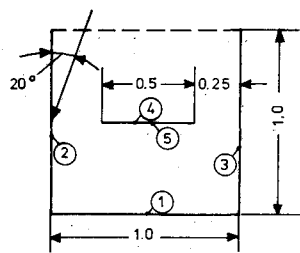
Numerical Results

Calculations were made for an open cone and an open cylinder. The surfaces were assumed black, diffusely reflecting and/or specularly reflecting; the number of trials varied between 1500 and 4000. The results agreed with those of Lin and Sparrow.¹⁴ The errors were in the order of magnitude as could be expected from Eq. (4). When using Gebhart's method¹⁰ to transform view factors into the absorption factors for the diffuse case, and when subdivision of

Table 1 Outline of computer program

- 1) Read in geometry and codes
- 2) Calculate in 4 loops the 6 matrices $V_{x, \max}(i, j), \dots$ that define how the surfaces face each other and calculate the normals to plane surfaces
- 3) Loop in which a case is defined (for the specified enclosure)
- 4) Read in surface properties and, if required, the surface representing the sun, and read direction of sunlight
- 5) Loop in which the radiating surface i is defined
- 6) Loop in which a particular ray is defined; calculation of its origin (with $R1$ and $R2$) and its direction (with $R3$ and $R4$)
- 7) Loop in order to look for the receiving surface j
- 8) Test if a point of impingement S of a ray on j is in principle possible by using Eqs. (2); if 'no' go to 14
- 9) Calculate S between the ray and the plane of j
- 10) Test if S is inside or outside j (by using Eqs. (3) first, if applicable); if 'outside' go to 14
- 11) Calculate the length of the vector V_{ij} from origin of ray to S ; test if a shorter $|V_{ij}|$ had already been found for another j ; select and register the shorter $|V_{ij}|$ and the corresponding j ; test if j is last surface of enclosure to be scanned; if 'no' go to 14
- 12) Decide whether the ray is absorbed or reflected (with $R5$); if 'absorbed,' register a counter in the element of the B_{ij} matrix and skip to 16; if 'reflected', calculate the new direction (with $R6$ and $R7$ in the case of diffuse reflection)
- 13) Surface j takes over the role of surface i , but the original surface i from which the radiation stems is registered
- 14) End of loop that starts at 7
- 15) No impingement at all has been found; the ray has left the enclosure and B_{is} is registered
- 16) End of loops that start at items 6 and 5
- 17) Print out B_{ij} matrix
- 18) End of loop that starts at item 3

Fig. 3 Enclosure with five surfaces receiving solar radiation.



the cavity is not fine enough, the resulting errors were much greater than those obtained with Monte Carlo.

Figure 3 shows a configuration of five surfaces. Surfaces 1 to 3 are three inner surfaces of a unit cube. Surfaces 4 and 5 are the two surfaces of a square lying parallel to surface 1, but having half the length of surfaces 1 to 3.

The B_{ij} factors were first calculated by assuming surfaces 4 and 5 to be nonexistent. Calculations were carried out for the black, diffuse, specular and mixed diffuse-specular cases. The tables of Hamilton and Morgan contain the exact results for the black case: $B_{12} = 0.20004$ and $B_{23} = 0.19982$. The Monte Carlo method gave values varying between 0.194 and 0.2087 for these factors and for those which are symmetrical (N between 1500 and 3000). The method of uniform rays mentioned previously gave $B_{12} = 0.2025$ and $B_{12} = 0.2002$ when 3×3 points and 5×5 points, respectively, were uniformly distributed over the surface (the number of rays per point was chosen such that in each case approximately the same computing effort was required as by Monte Carlo). The results of the method of uniform rays are closer to the exact ones. For the gray case, the results of the method of uniform rays showed greater scatter than those of Monte Carlo.

Then a calculation was made of the absorption of solar radiation incident under 20° by all five surfaces of Fig. 3. For that purpose an imaginary surface, indicated by the broken line, was assumed between the ends of surfaces 2 and 3. Rays of arbitrary origin but fixed direction started from this imaginary surface. The results are given in Table 2.

Rows 1 to 3 present the black case, and rows 4 to 6 the gray diffuse case. Row 1 can easily be obtained by geometrical considerations. Rows 3 and 6 present results for stratified sampling, i.e., subdivision of the solar surface in four sections. A comparison of rows 2 and 3 with row 1 shows good agreement; the subdivision brought about no noticeable improvement, however. Row 4 was found by calculating the 5×6 matrix of view factors, transforming these into the absorption factors and considering all interchanges. The results given in this row are not accurate due to the error of the finite size of the surfaces. Radiation from surface 1, for instance, strikes surface 2 mainly at the part nearest surface 1, and from this position the probability of the radiation being reflected back to 1 is greater than of being reflected through the

Table 2 Absorption factors for sun radiation (Fig. 3)

$\alpha = 1$						
$j = 1$	2	4				
0.386	0.364	0.25	; exact			
0.385	0.3601	0.2549	; $N = 10000$			
0.3854	0.3606	0.254	; $N = 4 \times 2500$			
$\alpha = 0.6, \rho_a = 0.4$						
$j = 1$	2	3	4	5	space	
0.256	0.2452	0.03971	0.1533	0.01677	0.289	; from row 1
0.2573	0.2622	0.0359	0.1552	0.0174	0.272	; $N = 10000$
0.2537	0.2611	0.036	0.1569	0.0140	0.2783	; $N = 4 \times 2500$

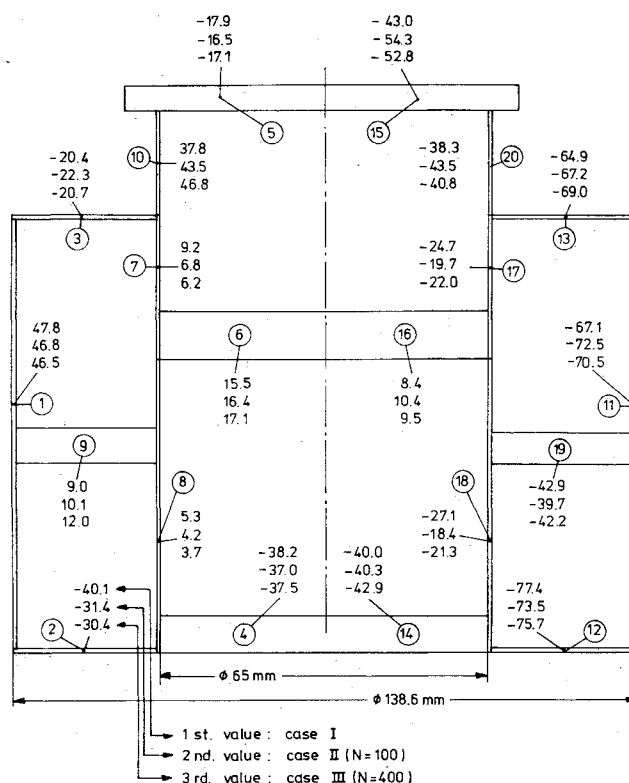


Fig. 4 Temperatures ($^\circ\text{C}$) of a 20-node model irradiated from the left-hand side.

imaginary surface to space (by assuming surfaces 4 and 5 to be nonexistent). This is not considered in the method of transforming view factors. Therefore, the fraction of solar radiation reflected back to space is too high (28.9% compared to 27.2% or 27.8%, respectively).

Figure 4 shows a longitudinal cut through the EX1 capsule, which was intended as a test satellite on the ELDO rocket in 1971. The temperatures had to be assessed roughly. The rotationally symmetrical capsule was divided into 20 nodes as shown in Fig. 4 (encircled numbers). In order to include extreme cases it was assumed that the solar radiation falls from the left onto a nonspinning capsule with 1.3 solar constant (one can assume that this value accounts for about 20% Earth-radiation and 10% albedo-radiation). Nodes 1 to 10 on the left-hand side represent, therefore, the 'hot half' and nodes 11 to 20 on the right-hand side the 'cold half.' Nodes 4, 14, 6, 16, 5, 15 are halves of disks and nodes 2, 12, 9, 19, 3 and 13 are halves of annular disks. The masses of the equipment are considered to be included in these nodes. The remaining nodes are halves of cylinders.

The temperatures were calculated with three sets of B_{ij} factors. Case I (or set I): the factors were determined as carefully as possible by making view factors algebra and by estimations. Case II: the factors were calculated roughly by Monte Carlo. The number of trials per area was $N = 100$. Case III: the factors were calculated more precisely by Monte Carlo with $N = 400$. The following assumptions were made for the temperature calculations: all absorptivities for solar radiation $\alpha = 0.6$, all emissivities $\epsilon = 0.8$, no conduction, 5W each internal power dissipation in nodes 4 and 14 and 30W each dissipation in nodes 6 and 16.

The calculated steady-state temperatures are also given in Fig. 4 for the preceding three cases. A rough error analysis was made in order to gain an impression of how precise these temperatures are. The results are presented in Table 3.

P is the probability that the error is not greater than ΔT .

These temperature errors were found by applying Eq. (4)

Table 3 Average temperature errors of the 20-node model

P %	ΔT °C		P %	ΔT °C	
	$N = 100$	$N = 400$		$N = 100$	$N = 400$
84.3	1.24	0.62	76.1	2.36	1.18
95.2	1.47	0.735	95.1	3.34	1.67
99.3	1.72	0.86	99.2	4.10	2.05

to the thermal model described by Fig. 4. First it was assumed that only one absorption factor at a time is wrong by a relative amount d as given by Eq. (4). The results are given in columns 2 and 3 of Table 3 for $N = 100$ and $N = 400$, respectively. Then it was assumed that the exchange factors to all surrounding nodes that are hotter than the node in question are increased by d , and that simultaneously all exchange factors to nodes that are colder than the node in question are decreased by d . These results (columns 4 to 6) are more pessimistic than those in the first case. For these calculations the average temperature difference between the nodes was chosen 40°C according to Fig. 4.

From Table 3 one can conclude that the Monte Carlo method with $N = 400$ is sufficient for practical problems of this kind. In the following, cases I and II are compared with case III ($N = 400$). From Fig. 4 the average deviation between cases I and III can be calculated as 3.24°C, whereas the average deviation between cases II and III is only 1.62°C. From this we can conclude that even a rough determination of B_{ij} factors by Monte Carlo ($N = 100$) gives temperatures nearer to those obtained by using Monte Carlo with more trials ($N = 400$) than is possible even after a careful determination of radiation exchange by other means.

The purpose of this last example was to show that in the case of more complex geometries it might be sufficient for the resulting temperatures to apply Monte Carlo with a low number of trials giving a reduction in computer time. For all examples described here, the runs on computer IBM 360/50H took at most 20 min.

Approximation for Complex Enclosures

An enclosure of a spacecraft can be quite complex. For instance, a cut normal to the main axis of a spacecraft could result in a picture as shown in Fig. 5. An inner cylinder or cone (a), an outer cylinder (b), a platform (c), and an end cover could form an enclosure in which equipment (d) is located. Such an enclosure can be subdivided by k imaginary walls. Figure 5 shows a possible subdivision in subenclosures I to IV by four walls W . Instead of calculating one $n \times n$

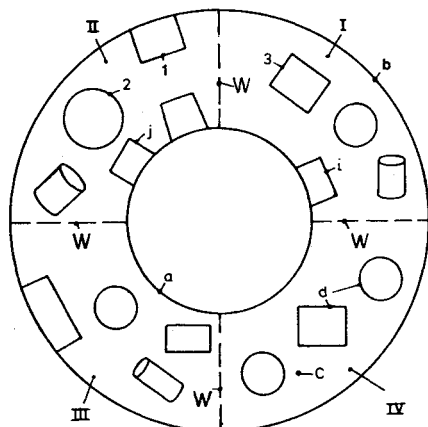


Fig. 5 Subdivision of an enclosure.

matrix of absorption factors for the whole enclosure, only k matrices, each in size $(n/k) \times (n/k)$ should be determined. The computing effort would be reduced by the factor $n^2/(kn^2/k^2) = k$. In the case of Fig. 5, where $k = 4$, the computer time would be only 25% of the time otherwise needed.

The calculation process should consist of three steps. First, calculate the reflectivities ρ and emissivities ϵ that should be used for the imaginary walls. Designate the two sides of the wall between the subenclosures I and II, for instance, in Fig. 5 by the superscripts ' and '' respectively. Calculate the absorption factors B'_{w-w} and B''_{w-w} (index w = wall) by using Monte Carlo in subenclosures I and II, respectively, and by taking the emissivities ϵ' and ϵ'' on the two sides of W first as unity. We can now write $\rho'_{w-w} = B'_{w-w}$ and $\rho''_{w-w} = B''_{w-w}$, where ρ'_{w-w} represents the probability, of a ray that enters from enclosure I through the wall W into enclosure II, being reflected back to I.

In the second step determine the B_{ij} factors in the different subenclosures by Monte Carlo, using the reflectivities and emissivities ($\epsilon'_{w-w} = 1 - \rho'_{w-w}$) of the imaginary walls.

In the third step, the connections between the enclosures are made. Let i designate a surface in I and j a surface in II (Fig. 5). B_{ij} is found by

$$B_{ij} = B'_{i-w} B''_{w-j} / (1 - B''_{w-w}) \quad (5)$$

B_{ji} can be calculated by interchanging in this equation the superscripts ' and '' and the indices i and j . B'_{i-w} is the probability of a ray emitted by i being absorbed by W . The radiation absorbed by W has to be distributed to the surfaces in enclosure II. This is included in the value B''_{w-j} . B''_{w-j} has to be divided by $1 - B''_{w-w}$ since a fraction of the radiation leaving W is reabsorbed by W ; this is already considered in B'_{i-w} . The sum $\sum_j B''_{w-j}$ gives just $1 - B''_{w-w}$, where the summation is made over all surfaces in II with the exception of W .

The method described is only an approximation, but the summation law is fulfilled in Eq. (5). The error is certainly negligible for those B_{ij} factors, of which i and j lie in the same subenclosure, as, for instance, surfaces 1 and 2 in Fig. 5. The error may be significant for those B_{ij} factors, for which i and j lie directly opposite each other but separated by an imaginary wall W , as, for instance, surfaces 1 and 3, because W does not receive the radiation diffusely from these surfaces, a necessary condition for the validity of the above method. For these pairs of surfaces, additional calculations are required by either using no walls at all and lumping some other surfaces together or by shifting the walls. However, this is only required for those B_{ij} factors which contribute significantly to over-all heat transfer.

Concluding Remarks

We have seen that Monte Carlo permits a formulation common to the absorption problem (absorption of radiation into a cavity), to the emission problem (emission out of a cavity), and to the interchange problem (interchange between surfaces). Special problems such as determining the directions in which incident radiation is reflected out of a cavity can be solved as well. The opening of the cavity is divided into several imaginary surfaces and the surfaces onto which the different incident rays are reflected are recorded.

The examples presented show that the Monte Carlo method eliminates the error caused by the finite size of the surfaces. A finer subdivision of the cavity, or an integration as required for other methods is therefore not necessary. The example of 20 nodes showed that there is practically no difference in the temperatures calculated by Monte Carlo for fewer (100) and more trials (400). This is explained by the fact that the greater absorption factors are usually determined with a higher precision than the smaller ones [see Eq. (4)]. A further explanation is that the summation law, $\sum_j B_{ij} = 1$, is

also fulfilled when the number of trials is low. Errors in net heat flows to each surface can, therefore, usually be expected to be much smaller than errors in particular absorption factors. The small number of trials, the techniques described, and the proposed subdivision of complex enclosures, all contribute to the reduction of computer time. This means that Monte Carlo can be applied for enclosures that are too complex for other methods. Consequently, we feel that Monte Carlo can and should play a more important role for radiation analysis in spacecraft than hitherto.

References

- ¹ Howell, J. R. and Siegel, R., "The Blackbody, Electromagnetic Theory, and Material Properties," *Thermal Radiation Heat Transfer*, Vol. I, NASA SP-164, 1968.
- ² Howell, J. R. and Siegel, R., "Radiation Exchange Between Surfaces and in Enclosures," *Thermal Radiation Heat Transfer*, Vol. II, NASA SP-164, 1969.
- ³ Eckert, E. R. G. and Sparrow, E. M., "Radiative Heat Exchange Between Surfaces With Specular Reflection," *International Journal of Heat & Mass Transfer*, Vol. 3, No. 1, 1961, pp. 42-54.
- ⁴ Sparrow, E. M., Eckert, E. R. G., and Jonsson, V. K., "An Enclosure Theory for Radiative Exchange Between Specularly and Diffusely Reflecting Surfaces," *Journal of Heat Transfer*, Vol. C84, 1962, pp. 294-300.
- ⁵ Bobco, R. P., "A Script-F Matrix Formulation for Enclosures With Arbitrary Surface Emission and Reflection Characteristics," *Journal of Heat Transfer*, Feb. 1971, pp. 33-40.
- ⁶ Weiner, M. M. et al., "Radiative Interchange Factors by Monte Carlo," ASME Paper 65-WA/HT-51, Nov. 1965.
- ⁷ Corlett, R. C., "Direct Monte Carlo Calculation of Radiative Heat Transfer in Vacuum," *Journal of Heat Transfer*, Vol. 88, No. 4, Nov. 1966, pp. 376-382.
- ⁸ Torr, J. S. and Viskanta, R., "A Numerical Experiment of Radiant Heat Interchange by the Monte Carlo Method," *International Journal of Heat & Mass Transfer*, Vol. 11, 1968, pp. 883-897.
- ⁹ Vossebrecker, H., "Zur Berechnung des Wärmetransportes durch Strahlung mit der Monte-Carlo-Methode," *Wärme- und Stoffübertragung*, Vol. 3, 1970, pp. 146-152.
- ¹⁰ Gebhart, B., *Heat Transfer*, 1st ed., McGraw-Hill, New York, 1961, pp. 117-122.
- ¹¹ Mize, J. H. and Cox, J. G., *Essentials of Simulation*, 1st ed., Prentice-Hall, Englewood Cliffs, N. J., 1968, pp. 70-73.
- ¹² Doenecke, J., "Thermal Radiations Absorbed by a Partially Obscured Spacecraft," *Astronautica Acta*, Vol. 15, 1969, pp. 107-117.
- ¹³ Hammersley, J. M. and Handscomb, D. C., *Monte Carlo Methods*, 1st ed., Methuen, London, 1964, pp. 55-66.
- ¹⁴ Lin, S. H. and Sparrow, E. M., "Radiant Interchange Among Curved Specularly Reflecting Surfaces—Application to Cylindrical and Conical Cavities," *Journal of Heat Transfer*, Vol. 87, No. 2, May 1965, pp. 299-307.